Potential Application of Fusarium Fungal Strains (Fusarium sp. FP, Arthrinium sp. FB and Phoma sp. FR) for Removal of Tl(I) Ions from Water

Jianying Mo (jianying_mo@163.com)
Guangdong Provincial Academy of Environmental Science https://orcid.org/0000-0003-2526-8663
Yonghui Liu
Guangzhou University
Xiaoning Gao
Institute of Bioengineering
Shuyi Zhou
Guangzhou University
Yirong Deng
Guangdong province academy of environmental science
Yanyang Ke
Guangzhou University
Lihu Peng
Guangzhou University
Huosheng Li
Guangzhou University
Sihao Chen
Guangzhou University
Jianyou Long
Guangzhou University

Research Article

Keywords: Removal, Thallium, Biosorption, Fungal strains, Mechanisms

Posted Date: November 9th, 2021

DOI: https://doi.org/10.21203/rs.3.rs-923922/v1

Version of Record: A version of this preprint was published at Environmental Science and Pollution Research on February 14th, 2022. See the published version at https://doi.org/10.1007/s11356-022-18791-1.

Potential Application of *Fusarium* Fungal Strains (*Fusarium sp.* FP, *Arthrinium sp.* FB and *Phoma sp*. FR) for Removal of Tl(I) Ions from Water

Jianying Mo[1,a,b,] Yonghui Liu[1,a,], Xiaoning Gao[c], Shuyi Zhou[a], Yirong Deng [b*] , Yanyang Ke[a], Lihu Peng, Huosheng Li [a], Sihao Chen[a], Jianyou Long [a,*]

[a]*School of Environmental Science and Engineering, Guangzhou University, Guangzhou 510006, China.*

[b]*Guangdong Provincial Academy of Environmental Science, Guangdong Key Laboratory of Contaminated Sites Environmental Management and Remediation and Guangdong-Hongkong-Macau Joint Laboratory of Collaborative Innovation for Environmental Quality, Guangzhou 510045, China*

[c]*Institute of Bioengineering, Guangdong Academy of Sciences, Guangzhou 510316, China*

[*] *Corresponding author: longjyou@gzhu.edu.cn (J. Long), ecoyrdeng@163.com.*

[1] *Jianying Mo and Yonghui Liu contributed equally to this work.*

Abstract: Water pollution caused by heavy metals poses a serious threat to the ecosystem and human survival safety and becomes a major obstacle to human health, economic and socially sustainable development. Among the various treatment techniques for water remediation, adsorption is an efficient method due to its high capacity, low cost, and simplicity. Thallium (Tl) is highly toxic to mammals and its removal from water is gaining increasingly prominent attention. In this study, three fungal strains (*Fusarium* sp. FP, *Arthrinium* sp. FB and *Phoma* sp. FR) were tested for removal of Tl(I) from an aqueous solution and showed excellent removal performance. The prepared inactive fungal strains were characterized by XRD, FT-IR, SEM, and XPS analysis. The effects of pH, contact time, biomass and reaction temperature on the removal efficiency of Tl(I) were systematically investigated. The results indicated that the adsorption isotherm data fit well with the Langmuir model, and the pseudo-second-order model was more consistent with the kinetic data description. The maximum adsorption capacity of the fungal strain (*Fusarium* sp. FP, *Arthrinium* sp. FB and *Phoma* sp. FR) for Tl(I) was found to be 94.69 mg/g, 66.97 mg/g and 52.98 mg/g, respectively. The thermodynamic data showed that the sorption process was spontaneous and endothermic. The present study showed that the inactive fungal strains could be a promising adsorbent material for Tl(I) removal.

Keywords: Removal, Thallium, Biosorption, Fungal strains, Mechanisms

* *Corresponding author.*

E-mail addresses: longjyou@gzhu.edu.cn (J. Long), ecoyrdeng@163.com.

Introduction

Water is important for all life organisms on earth. However, fresh water is no longer easily available due to unwanted toxic chemicals such as heavy metals (Dimpe &Nomngongo 2017). Among the various heavy metals, thallium (Tl) is more toxic to the ecosystem and human health than conventional heavy metals such as Cd, Cu, Hg, and Pb (Li et al. 2017, Peter &Viraraghavan 2005), and causes significantly adverse health effects even at a low level. Tl mainly exists in two oxidation states (Tl(I) and Tl(III)) in the aqueous environment (Li et al. 2019b, Wick S et all. 2018). Tl(I) is highly stable and mobile and thus dominant in water (Birungi &Chirwa 2015). While Tl(III) is highly reactive and can be easily hydrolyzed in alkaline or neutral solutions. Tl is widely used in the industries of optical lenses, alloys, dyes, rodenticides, semiconductors, and pigments (Wan, S et al. 2014). Long-term Tl poisoning can cause anorexia, headache, abdomen pains, alopecia, blindness and even death (Galván-Arzate &Santamaría 1998). To minimize these health risks, a maximum contaminant level of 2 μg/L was set as drinking water standard by the US Environmental Protection Agency (Zou Y et all. 2020). A much more stringent standard for the source of drinking water was established in China, in which the upper limit of Tl is 0.1 μg/L. This indicates that there is a great need to develop efficient methods for the Tl(I) treatment technology.

To date, various techniques have been investigated for the removal of Tl(I) wastewaters, including adsorption (Huosheng et al. 2020a, Huosheng et al.2020b, Li keke et al. 2020), oxidation (Li et al. 2019a, Liu et al. 2017), ion exchange (Hanafi 2010), and solvent extraction (Rajesh &Subramanian 2006). Among these techniques, adsorption is an attractive one due to its simple operability and high efficiency. A variety of adsorbents, such as carbon nanotubes (Pu et al. 2013), modified aspergillus niger biomass (Peter &Viraraghavan 2008), modified sugar beet pulp (Zolgharnein et al. 2011), activated carbon (Rivera-Utrilla et al. 1984), titanate nanotubes (Liu et al. 2014), MnO_2@pyrite cinder (Huosheng et al. 2018, Li et al. 2018), saw dust (Memon et al. 2008), microbial fuel cells (Wang et al. 2018), and amorphous hydrous manganese dioxide (Wan et al. 2014) have been tested for the removal of Tl(I) ions from water. There are abundant functional groups on the surface of microbial cell walls, such as sulfhydryl, hydroxyl, carboxyl and amide, whose complexation and coordination make both the active and inactive biomass of microorganisms exhibit a good ability to adsorb heavy metals. These groups can form covalent bonds with the adsorbed metal ions to achieve the purpose of adsorption removal. The usage of inactive biomass for heavy metal removal is more advantageous than active one owing to a variety of mechanisms such as complexation, electrostatic interactions, chelation ion exchange, non-toxicity concerns (Long et al. 2017). Other advantages of using inactive biomass as adsorbent are no requirement of growth media or nutrients. Therefore, the inactive biomass of microbes has become one of the prominent options among the adsorbents for the removal of Tl from wastewaters.

In this study, three different fungal strains (*Fusarium* sp. FP, *Arthrinium* sp. FB and *Phoma* sp. FR) were synthesized, characterized with XRD, SEM, and applied in Tl(I) removal from water. The Tl(I) removal mechanism was also explored by FT-IR and XPS analyses. Various operating parameters such as pH, adsorbent dosage, initial Tl(I) concentration, contact time, and reaction temperature, were evaluated systematically in batch experiments. In addition to kinetic and isotherm, thermodynamic parameters were also evaluated to understand the mechanism of removal Tl(I) ions with the adsorbent. The obtained results will be helpful for the development of low cost and eco-friendly sorbents for the removal of Tl(I) ions in feature.

Materials and methods

Chemicals and reagents

All chemicals and reagents used in the test were analytical grade and were used according to the provided standards (Guangzhou Huaxin reagent Co. Ltd). The water for the whole test process is obtained through the deionized water equipment (YL05-20L 75G, Shenzhen, China). A Tl(I) stock solution (1000 mg/L) was dissolved by $TINO_3$ (99.99%, Aldrich) in 2.0 mol/L HNO_3 solution. The working solution was serially diluted from standard solution when needed.

Preparation of adsorbents

The pure fungal colonies of different fungi were inoculated on sterilized Potato Dextrose Agar medium (PDA: peeled potato 200 g, glucose 20 g, deionized water 1000 ml, pH 6.8-7.0) and incubated at 25 ℃ in 250 mL triangle flasks on a temperature-controlled shaker at 150 r/min of agitation speed for the cultivation (72 h). After filtering and collecting the mycelium, the biomass was rinsed with deionized water several times for removing the residual medium and impurities, and dried in an oven at 100 ℃ for 2 h, and then ground into fine powder for the subsequent adsorption studies.

Phylogenetic analysis of the Tl(I)-resistant fungi

The genomic DNA of the thallium-tolerant fungal was extracted and then was polymerase chain reaction (PCR) amplified with the universal primers to amplify the ITS1-5.8S-ITS2 region sequence. The PCR product was analyzed by electrophoresis in 0.8% agarose gel and the objective gene fragment was collected and sent for gene sequencing at Shanghai Sangon Company. The obtained sequence was analyzed at Genebank database using BLAST program, and the aligned gene sequences of the related species were retrieved from the NCBI nucleotide database. The software Clustal X with default parameters was run for implementing the multiple sequence alignment. The phylogenetic tree was constructed using neighborhood joining method through 1000 repeated samplings, and the phylogenetic tree and genetic distance were analyzed by MEGA6.0 program.

Batch adsorption experiments

All batch adsorption experiments were conducted in a rotary shaker by using 100 mL Erlenmeyer flasks. The effect of pH solution on the removal of Tl(I) was studied at a certain concentration of Tl(I) with the pH range from 2.0 to 7.0. To investigate the effect, pH was adjusted by using 0.2 mol/L HCl or NaOH. To study the effect of contact time, adsorption experiments were carried out with 25 mL of 10 mg/L Tl(I) solutions. The suspensions were kept in contact for different times (30-240 min). For kinetic and isotherm studies, the initial concentration of Tl(I) varied from 10 to 150 mg/L and the solution pH was adjusted to 5. After contact for 60 min, the solution was filtered thrice using Whatman filter paper and then determined the concentration of residual Tl(I) ion through ICP-MS. All experiments were implemented in triplicate and the data were shown as the average values. The amount of Tl(I) adsorbed by the

sorbent was determined from the difference of Tl(I) concentrations in the initial and final solutions employing the following equation below:

$$q_e = \frac{(C_0 - C_e)\mathrm{V}}{M} \quad (1)$$

$$R(\%) = \frac{(C_0 - C_e)}{\mathrm{C_0}} \times 100 \quad (2)$$

where C_0 (mg/L) is the initial concentration of Tl(I), C_e (mg/L) is the equilibrium Tl (I) concentrations of the solutions, V (L) is the solution volume, and M is the mass (g) of adsorbent.

Characterization of the adsorbents

Fourier transform infrared (FT-IR) spectroscope (ALPHA-T, Bruker German) was used to analyze surface functional groups. The samples were prepared by mixing dried biomass with KBr with the mass ratio of 1:100, and spectra were recorded in the wave number range of 400-4000 cm^{-1}. The surface morphology and elemental composition of the pure fungal strains and Tl(I) loaded were observed through SEM and EDX (PANalytical, Neitherland). XPS analysis (Kratos Axis Ultra, Japan) was carried out to elucidate the adsorption mechanism of fungal strains with Tl(I) ion. The concentration of Tl(I) in the samples was measured by ICP-MS (Agilent, 7700, USA).

Results and discussions

Phylogenetic tree analysis of Tl(I)-resistant fungus

According to the phylogenetic tree analysis of 16S rRNA, the gene sequences of the isolated strain JCCW-FP, JCCW-FB and JCCW-FR have a 99% sequence identity to the members of the genus *Fusarium* sp., *Arthrinium* sp. and *Phoma* sp. (Figure 1), Based on which is named as Fusarium sp. FP, Arthrinium sp. FB and Phoma sp. FR, respectively. To the knowledge of existing documentation, the three isolated strains have been demonstrated as a high-efficiency approach for the removal of heavy metals, Cd (II), Pb (II) an so on (Anagnostopoulos et al. 2012), and may also be conceivable for the biosorption of other metals such as Tl(I).

XRD analysis

The inactive biomass of three strains before and after Tl(I) adsorption was determined by XRD analysis. The XRD analysis of pure Fusarium sp. FP, Arthrinium sp. FB Phoma sp. FR and Tl(I) loaded Fusarium sp. FP, Arthrinium sp. FB Phoma sp. FR were displayed in **Figure 2A-F.** The XRD patterns of three strains had a weak and broad at 2Θ=22˚ indicating that all the inactive biomasses of three strains were in low crystallinity. Comparted with the adsorbent before adsorption, and more intense peaks for the adsorbent after Tl(I) adsorption were observed, due to the presence of Tl(I)bonding with molecules that may lead to stronger crystallinity.

FT-IR analysis

The FT-IR spectra of pure fungal strains (Fusarium sp. FP, Arthrinium sp. FB Phoma sp. FR) and Tl(I) loaded fungal strains were shown in Figure 3. There was an obvious change in the intensity of the bands in FT-IR spectra of

the biomass after the adsorption of Tl(I) ions. The peak at 3392.10 cm^{-1} representing the stretching of -OH or $–NH_2$ groups shifted to 3404.89 cm^{-1} after adsorption for *Fusarium* sp. FP, from 3379.31 to 3398.87 cm^{-1} for *Arthrinium* sp. FB and from 3385.33 to 3425.20 cm^{-1} for *Phoma* sp. FR, respectively. This could result from the functional groups -OH or $–NH_2$ bonding with Tl(I) ions subsequently leading to the shift of stretching vibration of -OH or $–NH_2$ groups. Before Tl(I) sorption, the band peak corresponding to C=O stretching of amide was observed at 1630.09 and 1643.64 $cm^{–1}$ (Liao Q et all. 2020). The peaks at 1060.56 and 1034.23$cm^{–1}$ band were assigned to –H-C-H or C-O stretching vibrations (Huang J et all. 2021). After Tl(I) adsorption, a change in peak positions as described above shifted from 1630.09 to 1650.41 cm^{-1} and 1060.56 to 1074.11 cm^{-1} for *Fusarium* sp. FP, from 1636.87 to 1656.43 cm^{-1} and 1041 to 1053.79 cm^{-1} for *Arthrinium* sp. FB, 1643.64 to 1624.08 cm^{-1} and 1034.23 to 1047.71 cm^{-1} for *Phoma* sp. FR, respectively, demonstrating that the involvement of C=O, C-O and –CH groups in Tl (I) adsorption process (Anton L et all. 2013).

SEM with EDS analysis

The scanning electron microscopy was used to understand the variation in morphological features and surface characteristics of the adsorbent material. The elemental distribution over the surface is confirmed by EDS analysis. The SEM with EDS micrographs of the three inactive strains before and after Tl(I) adsorption were depicted in Figure 4. Before adsorption, the surface of the adsorbent was relatively smooth. After adsorption, the surface became rough. Thus, distinctive changes in the inactive surface of three strains were observed before and after Tl(I) adsorption. Through the EDS analysis of the adsorbent sample after Tl(I) adsorption, peaks of Tl(I) ion were observed along with all the other components identified in the adsorbent, which might be due to the adsorption of Tl(I) ions(Bulut Y et all. 2006).

XPS analysis

The chemical states of the surface elements of fungal strains of *Fusarium* sp. FP, *Arthrinium* sp. FB and *Phoma* sp. FR were further determined with XPS measurements and shown in Figure 5. As illustrated in Figure (5a, 6a, 7a), a wide scan spectrum comprised of carbon, nitrogen and oxygen. After the Tl(I) sorption, Figure 5b, 6b, 7b showed a new peak and it represents the Tl 2d spectra. This result confirms that the Tl(I) ions were successfully sorbed by the three bacterial strains. The deconvolution of C1s spectra produces three peaks with binding energy of 284.2, 285.6 and 287.8 eV. As shown in Figure 5c, 6c, 7c, these peaks can be allocated to the C atom in the form of C-C, C-OH, O=C-O, respectively(Li Y et all. 2018). After the Tl (I) sorption, the content of C increased from 75.82% to 80.32% for *Fusarium* sp. FP, 74.94% to 77.21% for *Arthrinium* sp. FB and 70.82% to 73.21% for *Phoma* sp. FR. The peak at 398.4 eV mainly belongs to $R\text{-}NH_2/R_2\text{-}NH$ group(Ho Y-S et all. 1999). It can be seen from Fig.7c and Fig.7d that the peak area percentage decreased from 8.1% to 6.8%. The $R\text{-}NH_2/R_2\text{-}NH$ group participated in the Tl(I) sorption causing a significant reduction in its relative content. As to the peak at binding energy of 528.45 eV, the increment of peak area percentage indicated that C=O groups contributed to the removal of Tl(I) ions from aqueous solution. The conclusions obtained were consistent with the ft-IR experimental results.

Influence of pH

The effect of pH on the adsorption of Tl(I) onto fungal strains (*Fusarium* sp. FP, *Arthrinium* sp. FB and *Phoma* sp. FR) was investigated by using 25 mL of Tl(I) (100 and 200 mg/L) for a pH range of 2.0 to 8.0 at room temperature, as shown in Figure 8A. It is clear that the uptake of Tl(I) tends to increase with increasing pH (2.0 to 5.0) and reaches to the maximum value at pH 5.0. When the pH values were below 3.0, there was a lower Tl(I) removal efficiency because at these lower pH values, Tl(I) ions had to compete with H_3O^+ ions for the sorption sites. In acidic media, H^+ ions could not only protonate amine and hydroxyl groups generating strong electrostatic repulsion towards Tl(I) but also compete with Tl(I) for adsorption sites(Galván-Arzate S et all. 1998). Hence, the removal efficiency of Tl by fungal strains was poor at low pH values. The optimal removal efficiency of Tl(I) ions occurred at pH 5.0. Further, all the subsequent sorption experiments of Tl(I) ions were operated under the optimal pH value of 5.0.

Influence of biomass dosage

The amount of adsorbent used in adsorption is important because it determines the sorbent–sorbate equilibrium and can also be used to predict the treatment cost of adsorbent per unit of Tl(I) ions. The effect of adsorbent dosage on Tl(I) ions removal was studied from 0.5 to 3 g/L and the results were represented in Figure. 8B. The results show that removal of l % of Tl(I) ions decreased with increasing adsorbent dosage. It indicates that Tl(I) sorption onto biomass is not strictly a surface phenomenon and that some sorption sites may remain unsaturated during the sorption process due to possible electrostatic interactions between binding sites, ineffective mixing of metal solutions, and high sorbent dosages (Bulut &Baysal 2006, Rao &Khan 2009, Sharma &Forster 1993). Maximum Tl(I) adsorption capacity of 63.75 mg/g for *Fusarium* sp. FP, 51.23 mg/g for *Arthrinium* sp. FB and 49.80 mg/g for *Phoma* sp. FR were obtained when 0.5 g/L of biomass was used.

Influence of initial Tl(I) concentration

Initial concentration provides an important driving force to overcome mass transfer resistances between the aqueous and solid phases (Dönmez, G., & Aksu, Z.2002). In the present study, initial Tl(I) concentration varied from 10-300 mg/L and the results are shown in Figure 8C. The sorption capacity increased with increasing Tl(I) concentration and then reached almost constant value. The initial increase in sorption capacity may be owing to higher availability of Tl(I) ions. Moreover, a high concentration enables a driving force to overcome the mass transfer resistance between Tl(I) ions and adsorbents. No considerable increase in the sorption capacity with further increase in Tl(I) concentration suggests the saturation of binding sites(Huangfu X et all. 2017).

Influence of contact time

In the intermittent adsorption process, contact time is one of the effective factors. All of the parameters except contact time, including temperature, adsorbent dose (10 g/L), pH (5), initial Tl(I) concentration (100 mg/L) and agitation speed (160 rpm), were kept constant, and the results were depicted in Figure 8D. The adsorption capacity for the three biomasses reached equilibrium at 60 min, and the maximum adsorption capacity was found to be 63.86 mg/g for *Fusarium* sp. FP, 53.21 mg/g for *Arthrinium* sp. FB and 49.50 mg/g for *Phoma* sp. FR, respectively. In the initial stages, the metal removal efficiencies of adsorbents increased rapidly due to abundant availability of active

binding sites on the biomass, and gradually these sites would be occupied by Tl(I) ions. Afterward, it continued at a slower rate and finally reached equilibrium when the adsorption sites on the adsorbent surface reached saturation.

The adsorption became less efficient in the later stages and finally it reached equilibrium(Li H et all. 2017). The contact time of 60 min was found to be sufficient to reach equilibrium, so it was selected as the optimum time for the further experiments.

Adsorption kinetics

Kinetic study is important in batch experiments to optimize the contact time and to know the kinetic model that the adsorption is following. The pseudo-first-order kinetic (Lagergren 1898) and pseudo-second-order kinetic (Ho &McKay 1999) were used to evaluate the adsorption data of Tl(I) ions.

The pseudo-first-order model describes the relationship between the adsorption rate on adsorbent and the equilibrium time. The linear form of the pseudo-first-order kinetic model can be expressed as follows:

$$\log(q_e - q_t) = \log q_e - \frac{k_1 t}{2.303} \quad (3)$$

Where q_e (mg/g) represents the adsorption capacity at equilibrium of the solutions, q_t (mg/g) represents the adsorption capacity at time (h) t, k_1 (h^{-1}) represents the rate constant at equilibrium.

The pseudo-second-order model was based on the assumption that the adsorption rate is controlled by the chemical adsorption mechanism, and this chemical adsorption involves electron sharing or electron transfer between adsorbent and adsorbate.(Wu.Q et all. 2018) The linear form of the pseudo-second-order kinetic model can be expressed as follows (Sarı, A. et all. 2011):

$$\frac{t}{q_t} = \frac{1}{k_2 q_e^2} + \frac{t}{q_e} \quad (4)$$

Where q_e (mg/g) represents the adsorption capacity at equilibrium, q_t (mg/g) represents the adsorption capacity at the time (h) t, and k_2 (g/mg/ h) is the second-order rate constant of the adsorption process. The pseudo-first-order and pseudo-second-order kinetic rate constant K_1, K_2 and q_e values were determined from the slope and intercept of Figure 8E, and the related calculated parameters were summarized in Table 1. The correlation coefficients for the pseudo-first-order kinetic constants were much lower than the pseudo-second-order kinetic model. As seen from the Table 1, the calculated q_e values of pseudo-first-order were too low compared with experimental q_e values in all experiments. Whereas the calculated q_e values of pseudo-second-order model fitted well with the experimental data better than the pseudo-first-order kinetic model(Li H et all. 2018). This suggests that the pseudo-second-order adsorption was more appropriate to describe the overall rate of Tl(I) adsorption process, which appeared to be controlled by chemical sorption process(Li H et all. 2019b).

Adsorption isotherms

Adsorption isotherms describe the adsorption capacity of the adsorbent versus the concentration of the adsorbate at equilibrium. The Langmuir model assumes that the adsorption process occurs on a uniform surface through a single layer, and there is no interaction between the adsorbed ions. In this study, the experimental data was analyzed using the widely used Langmuir (Langmuir 1918) and Freundlich isotherm (Freundlich 1907) models and the Langmuir isotherm was shown in Figure 8F and the values were demonstrated in Table 2. The linear form of the Langmuir equation can be expressed as follows:

$$\frac{C_e}{q_e} = \frac{1}{Q_{max}b} + \frac{C_e}{Q_{max}} \quad (5)$$

where q_e (mg/g) is the adsorption capacity of Tl(I), C_e (mg/L) is the equilibrium concentration of Tl(I), Q_{max} (mg/g) is the saturated monolayer maximum adsorption capacity and b (L/mg) is the Langmuir isotherm constant that relates to the energy of adsorption. At the point of maximum adsorption, only a monolayer of adsorbate is formed and there is no interaction between sorbed molecules.

The Freundlich model assumes that the uptake of metal ions takes place on heterogeneous surfaces, and adsorption capacity is related to the concentration of the metal ions at equilibrium. The equation can be represented by the following formula(Li H et all. 2020):

$$logq_e = logK_f + \frac{1}{n}logC_e \quad (6)$$

where q_e (mg/g) is the adsorption capacity, C_e (mg/L) is the equilibrium concentration of the study solutions, K_f is the Freundlich constant related to the adsorption amount, n is the adsorption intensity of adsorption. It was found that the maximum sorption capacities of the synthesized fungal strains of *Fusarium* sp. FP, *Arthrinium* sp. FB and *Phoma* sp. FR were found to be 94.69 mg/g, 66.97 mg/g and 52.98 mg/g, respectively. Values of correlation coefficients (R^2) of the Langmuir isotherm were found to be 0.9825, 0.9687 and 0.9775 for the *Fusarium* sp. FP, *Arthrinium* sp. FB and *Phoma* sp. FR, respectively, at the tested temperatures and indicated that the Langmuir adsorption model fitted the equilibrium data very well. The R^2 values obtained by Freundlich isotherm fitting were low (0.9133, 0.9274 and 0.9195), which indicates that they were in poor agreement with Freundlich isotherm. The good fit of experimental data by the Langmuir equation confirms that the Tl(I) adsorption by the sorbent material in this study could be considered as homogeneous, because the possibility to sorb the target sorbate through the homogenous distribution of active site onto the surface(Padmavathy V et all. 2003). Based on the above facts, it may be concluded that compared to the Freundlich isotherm, the Langmuir isotherm is more consistent with experimental data.

Thermodynamic studies

Various thermodynamic parameters like enthalpy change (ΔH^o), entropy change (ΔS^o) and Gibbs free energy (ΔG^o) give the insights into the sorption mechanism. Enthalpy is the total heat of the system whereas the entropy measures the degree of randomness of the system (Lu et al. 2013). Entropy is the driving force for adsorption when the system is isolated and no heat transfer occurs from the system to the environment and vice versa (Igberase et al. 2014). The thermodynamic parameters can be calculated from the following Van't Hoff's equations:

$$\ln k_d = \frac{\Delta S^0}{R} - \frac{\Delta H^0}{RT} \quad (7)$$

$$\Delta G^0 = \Delta H^0 - T\Delta S^0 \quad (8)$$

Where K_d represents K and it is the thermodynamic equilibrium constant without unit. R is the gas constant (8.314 J/moL/ K), T is the absolute temperature in Kelvin. The values of ΔG^0, ΔH^0 and ΔS^0 were listed in Table 3.

The positive value of ΔH^0 showed that the adsorption process was endothermic in nature. (Pang C et al. 2010)The negative value of ΔG^0 confirmed that the adsorption process was feasible and spontaneous (Saravanan A et all. 2021). The negative values of ΔG^0 decreased with increasing temperature indicating that the adsorption became less favorable at higher temperatures. The positive value of ΔS^0 shows the increasing randomness between the sorbents and sorbate of the solution(Rong Pana et al. 2009).

Removal mechanisms

On this basis, a novel hybrid process, including complexation, Electrostatic interaction and adsorption, was proposed. The proposed mechanisms for Tl(I) removal by the strains were shown in Fig. 9. Firstly, Tl(I) diffused from the solution to the solid/water interface. Tl(I) ions then passed through the liquid film to the strain cell surface. -OH, NH_2 and NH groups on the surface of the strain were replaced by partial Tl(I), consequently. Meanwhile, partial Tl(I) were adsorbed by surface electrostatic adsorption and surface complexation.

Comparison study of inactive fungal strains with other sorbents

The maximum monolayer adsorption capacity (q_{max}) of fungal stains (*Fusarium* sp. FP, *Arthrinium* sp. FB and *Phoma* sp. FR) for the removal of Tl(I) ions was compared with that of other adsorbents reported in the literature (Memon et al. 2008, Sangvanich et al. 2010, Şenol &Ulusoy 2010, Vincent et al. 2014) and the values (pH, and q_{max}) were shown in Table 4. From the above results, it may conclude that fungal stains (*Fusarium* sp. FP, *Arthrinium* sp. FB and *Phoma* sp. FR) can act as a promising adsorbent for removal of Tl(I) ions from aqueous environment.

Conclusions

The efficiency of the synthesized fungal strains (*Fusarium* sp. FP, *Arthrinium* sp. FB and *Phoma* sp. FR) were studied for the removal of Tl(I) ion from aqueous solutions. Using Langmuir and the quasi-second-order kinetic model for fitting could accurately describe the Tl(I) adsorption isotherm and kinetic data, respectively. Based on the Langmuir isotherm model, the maximum adsorption capacity of fungal strains of *Fusarium* sp. FP, *Arthrinium* sp. FB and *Phoma* sp. FR were found to be 94.69 mg/g, 66.97 mg/g and 52.98 mg/g at equilibrium time of 60 min and 323 K, respectively. As shown in the above summary, the negative values of Gibbs free energy change and positive values of enthalpy change indicated that the adsorption nature of Tl(I) sorption onto the fungal strains adsorbents were feasible, spontaneous and endothermic.

Author contribution

All authors contributed to the study conception and design. Material preparation, data collection and analysis were performed by Jianying Mo, Yonghui Liu, Xiaoning Gao, Shuyi Zhou, Yirong Deng , Yanyang Ke, Lihu Peng, Huosheng Li, Sihao Chen and Jianyou Long. The first draft of the manuscript was written by Jianying Mo and Jianyou Long, and all authors commented on previous versions of the manuscript. All authors read and approved the final manuscript.

Funding

The study was supported by the National Natural Science Foundation of China (41370028, U1911202), Guangdong innovation platform characteristic innovation project (2016KTSCX106), GDAS Project of Science and Technology Development (2019GDASYL-0103029), the Fundamental and Applied Fundamental Research Major Program of Guangdong Province(2019B030302013) , Guangzhou city science and technology project (201804010281) and Guangdong Natural Science Foundation (2018A0303130265).

Declarations

Ethical Approval and Consent to Participate

Not applicable

Consent to Publish

Not applicable

Competing Interests

The authors declare that they have no competing interests

Availability of data and materials

The datasets used and/or analysed during the current study are available from the corresponding author on reasonable request.

References

Anagnostopoulos, Vasileios A, MANARIOTIS, Ioannis D, KARAPANAGIOTI, Hrissi K, CHRYSIKOPOULOS, Constantinos V (2012): Removal of mercury from aqueous solutions by malt spent rootlets. Chemical Engineering Journal 213, 135-141. https://doi.org/10.1016/j.cej.2012.09.074

Anton L, Antonia M, Somoano D, Mercedes, Tarazona M, Rosa M, Spears, Alan D (2013): Thallium in coal: Analysis and environmental implications. Fuel 105, 13-18. https://doi.org/10.1016/j.fuel.2012.08.004

Birungi Z, Chirwa E (2015): The adsorption potential and recovery of thallium using green micro-algae from eutrophic water sources. Journal of hazardous materials 299, 67-77. https://doi.org/10.1016/j.jhazmat.2015.06.011

Bulut Y, Baysal Z (2006): Removal of Pb (II) from wastewater using wheat bran. Journal of environmental management 78, 107-113. https://doi.org/10.1016/j.jenvman.2005.03.010

Dönmez, G., & Aksu, Z. (2002). Removal of chromium (VI) from saline wastewaters by Dunaliella species. Process biochemistry, 38(5), 751-762.https://doi.org/10.1016/S0032-9592(02)00204-2

Dimpe KM, Nomngongo PN (2017): A review on the efficacy of the application of myriad carbonaceous materials for the removal of toxic trace elements in the environment. Trends in Environmental Analytical Chemistry 16, 24-31. https://doi.org/10.1016/j.teac.2017.10.001

Freundlich H (1907): Über die adsorption in lösungen. Zeitschrift für physikalische Chemie 57, 385-470

Galván-Arzate S, Santamaría A (1998): Thallium toxicity. Toxicology letters 99, 1-13.

Hanafi A (2010): Adsorption of cesium, thallium, strontium and cobalt radionuclides using activated carbon. J At Mol Sci 1, 292-300. https://doi.org/10.1016/j.biortech.2014.01.012

Ho Y-S, McKay G (1999): Pseudo-second order model for sorption processes. Process biochemistry 34, 451-465. https://doi.org/10.1016/S0032-9592(98)00112-5

Huangfu X, Ma C, Ma J, He Q, Yang C, Zhou J, Jiang J, Wang Y (2017): Effective removal of trace thallium from surface water by nanosized manganese dioxide enhanced quartz sand filtration. Chemosphere 189, 1-9. https://doi.org/10.1016/j.chemosphere.2017.09.039

Huang, J., Liu, C., Price, G. W., Li, Y., & Wang, Y. (2021). Identification of a novel heavy metal resistant Ralstonia strain and its growth response to cadmium exposure. Journal of Hazardous Materials, 416, 125942. https://doi.org/10.1016/j.jhazmat.2021.125942

Huosheng L, Xiuwan L, Yongheng C, Jianyou L, Gaosheng Z, Tangfu X, Ping Z, Changlin L, Lingzhi Z, Wenyu H (2018): Removal and recovery of thallium from aqueous solutions via a magnetite-mediated reversible adsorption-desorption process. Journal of Cleaner Production. https://doi.org/10.1016/j.jclepro.2018.07.178

Igberase E, Osifo P, Ofomaja A (2014): The adsorption of copper (II) ions by polyaniline graft chitosan beads from aqueous solution: equilibrium, kinetic and desorption studies. Journal of Environmental Chemical Engineering 2, 362-369. https://doi.org/10.1016/j.jece.2014.01.008

Lagergren S (1898): Zur theorie der sogenannten adsorption geloster stoffe. Kungliga svenska vetenskapsakademiens. Handlingar 24, 1-39

Langmuir I (1918): The adsorption of gases on plane surfaces of glass, mica and platinum. Journal of the American Chemical society 40, 1361-1403

Liao, Q., Tang, J., Wang, H., Yang, W., He, L., Wang, Y., & Yang, Z. (2020). Dynamic proteome responses to sequential reduction of Cr (VI) and adsorption of Pb (II) by Pannonibacter phragmitetus BB. Journal of hazardous materials, 386, 121988. https://doi.org/10.1016/j.jhazmat.2019.121988

Li H, Chen Y, Long J, Jiang D, Liu J, Li S, Qi J, Zhang P, Wang J, Gong J (2017): Simultaneous removal of thallium and chloride from a highly saline industrial wastewater using modified anion exchange resins. Journal of hazardous materials 333, 179-185. https://doi.org/10.1016/j.jhazmat.2017.03.020

Li H, Li X, Xiao T, Chen Y, Long J, Zhang G, Zhang P, Li C, Zhuang L, Li K (2018): Efficient removal of thallium (I) from wastewater using flower-like manganese dioxide coated magnetic pyrite cinder. Chemical Engineering Journal 353, 867-877. https://doi.org/10.1016/j.cej.2018.07.169

Li H, Li X, Long J, Li K, Chen Y, Jiang J, Chen X, Zhang P (2019a): Oxidation and removal of thallium and organics from wastewater using a zero-valent-iron-based Fenton-like technique. Journal of Cleaner Production 221, 89-97. https://doi.org/10.1016/j.jclepro.2019.02.205

Li H, Xiong J, Xiao T, Long J, Wang Q, Li K, Liu X, Zhang G, Zhang H (2019b): Biochar derived from watermelon rinds as regenerable adsorbent for efficient removal of thallium (I) from wastewater. Process Safety and Environmental Protection 127, 257-266. https://doi.org/10.1016/j.psep.2019.04.031

Liu W, Zhang P, Borthwick AG, Chen H, Ni J (2014): Adsorption mechanisms of thallium (I) and thallium (III) by titanate nanotubes: ion-exchange and co-precipitation. Journal of colloid and interface science 423, 67-75. https://doi.org/10.1016/j.jcis.2014.02.030

Liu Y, Wang L, Wang X, Huang Z, Xu C, Yang T, Zhao X, Qi J, Ma J (2017): Highly efficient removal of trace thallium from contaminated source waters with ferrate: Role of in situ formed ferric nanoparticle. Water research 124, 149-157. https://doi.org/10.1016/j.watres.2017.07.051

Li, H., Xiong, J., Zhang, G., Liang, A., Long, J., Xiao, T., Chen, Y., Zhang, P., Liao, D., Lin, L. and Zhang, H. (2020) Enhanced thallium(I) removal from wastewater using hypochlorite oxidation coupled with magnetite-based biochar adsorption. Sci. Total Environ. 698, 134166. https://doi.org/10.1016/j.scitotenv.2019.134166

Li, K., Li, H., Xiao, T., Zhang, G., Liang, A., Zhang, P., Lin, L., Chen, Z., Cao, X. and Long, J. (2020) Zero-valent manganese nanoparticles coupled with different strong oxidants for thallium removal from wastewater. Frontiers of Environmental Science & Engineering 14(2), 34. https://doi.org/10.1007/s11783-019-1213-5

Li, Y., Li, L., Chen, T., Duan, T., Yao, W., Zheng, K., ... & Zhu, W. (2018). Bioassembly of fungal hypha/graphene oxide aerogel as high performance adsorbents for U (VI) removal. Chemical Engineering Journal, 347, 407-414. https://doi.org/10.1016/j.cej.2018.04.140

Li, Y., Li, H., Liu, F., Zhang, G., Xu, Y., Xiao, T., Long, J., Chen, Z., Liao, D., Zhang, J., Lin, L. and Zhang, P. (2020) Zero-valent iron-manganese bimetallic nanocomposites catalyze hypochlorite for enhanced thallium(I) oxidation and removal from wastewater: Materials characterization, process optimization and removal mechanisms. J. Hazard. Mater. 386, 121900. https://doi.org/10.1016/j.jhazmat.2019.121900

Long J, Li H, Jiang D, Luo D, Chen Y, Xia J, Chen D (2017): Biosorption of strontium (II) from aqueous solutions by Bacillus cereus isolated from strontium hyperaccumulator Andropogon gayanus. Process Safety and Environmental Protection 111, 23-30. https://doi.org/10.1016/j.psep.2017.06.010

Lu Y, He J, Luo G (2013): An improved synthesis of chitosan bead for Pb (II) adsorption. Chemical engineering journal 226, 271-278. https://doi.org/10.1016/j.cej.2013.04.078

Memon SQ, Memon N, Solangi AR (2008): Sawdust: a green and economical sorbent for thallium removal. Chemical Engineering Journal 140, 235-240. https://doi.org/10.1016/j.cej.2007.09.044

Pang, C., Liu, Y., Cao, X., Hua, R., Wang, C., & Li, C. (2010). Adsorptive removal of uranium from aqueous solution using chitosan-coated attapulgite. Journal of radioanalytical and nuclear chemistry, 286(1), 185-193. https://doi.org/10.1007/s10967-010-0635-0

Padmavathy V, Vasudevan P, Dhingra S (2003): Biosorption of nickel (II) ions on Baker's yeast. Process Biochemistry 38, 1389-1395. https://doi.org/10.1016/S0032-9592(02)00168-1

Peter AJ, Viraraghavan T (2005): Thallium: a review of public health and environmental concerns. Environment international 31, 493-501. https://doi.org/10.1016/j.envint.2004.09.003

Peter AJ, Viraraghavan T (2008): Removal of thallium from aqueous solutions by modified Aspergillus niger biomass. Bioresource technology 99, 618-625. https://doi.org/10.1016/j.biortech.2006.12.038

Pu Y, Yang X, Zheng H, Wang D, Su Y, He J (2013): Adsorption and desorption of thallium (I) on multiwalled carbon nanotubes. Chemical engineering journal 219, 403-410. https://doi.org/10.1016/j.cej.2013.01.025

Rajesh N, Subramanian M (2006): A study of the extraction behavior of thallium with tribenzylamine as the extractant. Journal of hazardous materials 135, 74-77. https://doi.org/10.1016/j.jhazmat.2005.10.057

Rao RAK, Khan MA (2009): Biosorption of bivalent metal ions from aqueous solution by an agricultural waste: Kinetics, thermodynamics and environmental effects. Colloids & Surfaces A Physicochemical & Engineering Aspects 332, 121-128. https://doi.org/10.1016/j.colsurfa.2008.09.005

Rivera-Utrilla J, Ferro-Garcia M, Mata-Arjona A (1984): 159. Adsorption studies of strontium on activated carbons from aqueous solutions. Carbon 22, 221-222.

Rong Pana, Lixiang Caob, Renduo Zhang(2009): Combined effects of Cu, Cd, Pb, and Zn on the growth and uptake of consortium of Cu-resistant Penicillium sp. A1 and Cd-resistant Fusarium sp. A19. Journal of Hazardous Materials 171, 761–766. https://doi.org/10.1016/j.jhazmat.2009.06.080

Sangvanich T, Sukwarotwat V, Wiacek RJ, Grudzien RM, Fryxell GE, Addleman RS, Timchalk C, Yantasee W (2010): Selective capture of cesium and thallium from natural waters and simulated wastes with copper ferrocyanide functionalized mesoporous silica. Journal of hazardous materials 182, 225-231. https://doi.org/10.1016/j.jhazmat.2010.06.019

Saravanan, A., Kumar, P. S., Govarthanan, M., George, C. S., Vaishnavi, S., Moulishwaran, B., ... & Yaashikaa, P. R. (2021). Adsorption characteristics of magnetic nanoparticles coated mixed fungal biomass for toxic Cr (VI) ions in aquatic environment. Chemosphere, 267, 129226.https://doi.org/10.1016/j.chemosphere.2020.129226

Şenol ZM, Ulusoy U (2010): Thallium adsorption onto polyacryamide–aluminosilicate composites: a Tl isotope tracer study. Chemical Engineering Journal 162, 97-105. https://doi.org/10.1016/j.cej.2010.05.005

Sarı, A., Uluozlü, Ö. D., & Tüzen, M. (2011). Equilibrium, thermodynamic and kinetic investigations on biosorption of arsenic from aqueous solution by algae (Maugeotia genuflexa) biomass. Chemical Engineering Journal, 167(1), 155-161. https://doi.org/10.1016/j.cej.2010.12.014

Sharma D, Forster C (1993): Removal of hexavalent chromium using sphagnum moss peat. Water Research 27, 1201-1208. https://doi.org/10.1016/0043-1354(93)90012-7

Vincent T, Taulemesse J-M, Dauvergne A, Chanut T, Testa F, Guibal E (2014): Thallium (I) sorption using Prussian blue immobilized in alginate capsules. Carbohydrate polymers 99, 517-526. https://doi.org/10.1016/j.carbpol.2013.08.076

Wan S, Ma M, Lv L, Qian L, Xu S, Xue Y, Ma Z (2014): Selective capture of thallium (I) ion from aqueous solutions by amorphous hydrous manganese dioxide. Chemical Engineering Journal 239, 200-206. https://doi.org/10.1016/j.cej.2013.11.010

Wick, S., Baeyens, B., Marques Fernandes, M., & Voegelin, A. (2017). Thallium adsorption onto illite. Environmental science & technology, 52(2), 571-580. https://doi.org/10.1021/acs.est.7b04485

Wu, Q., Xian, Y., He, Z., Zhang, Q., Wu, J., Yang, G., ... & Long, L. (2019). Adsorption characteristics of Pb (II) using biochar derived from spent mushroom substrate. Scientific reports, 9(1), 1-11. https://doi.org/10.1038/s41598-019-52554-2

Wang Z, Zhang B, Jiang Y, Li Y, He C (2018): Spontaneous thallium (I) oxidation with electricity generation in single-chamber microbial fuel cells. Applied Energy 209, 33-42. https://doi.org/10.1016/j.apenergy.2017.10.075

Zolgharnein J, Asanjarani N, Shariatmanesh T (2011): Removal of thallium (I) from aqueous solution using modified sugar beet pulp. Toxicological & Environmental Chemistry 93, 207-214. https://doi.org/10.1080/02772248.2010.523424

Zou, Y., Cheng, H., Wang, H., Huang, R., Xu, Y., Jiang, J., ... & Ma, J. (2020). Thallium (I) oxidation by permanganate and chlorine: kinetics and manganese dioxide catalysis. Environmental science & technology, 54(12), 7205-7216. https://doi.org/10.1021/acs.est.0c00068

467 **Table 1.** Kinetic parameters for the biosorption of Tl(I) ions onto Fusarium sp. FP, Arthrinium
468 sp. FB and Phoma sp. FR, respectively.

469

Biosorbent	Pseudo-first-order			Pseudo-second-order		
	q_e	K_1	R^2	q_e	K_2	R^2
FP	48.35	0.3328	0.90237	58.28	0.0139	0.9799
FB	43.74	0.1192	0.9136	51.97	0.0272	0.9773
FR	40.43	0.0754	0.9315	47.63	0.0243	0.9675

470

471

472 **Table 2.** Langmuir and Freundlich isotherm constants for the for the biosorption of Tl(I) ions
473 onto Fusarium sp. FP, Arthrinium sp. FB and Phoma sp. FR, respectively.

474

Biosorbent	**Langmuir Isotherm**			**Freundlich isotherm**		
	q_{max} (mg/g)	**K(L/mg)**	**R^2**	**K_f (mg/g)**	**n**	**R^2**
FP	94.69	0.2209	0.9825	2.3682	1.2946	0.9133
FB	66.97	0.1861	0.9687	1.9867	1.2574	0.9274
FR	52.98	0.1927	0.9775	1.5643	1.1968	0.9195

475

476

477

478

479

480 **Table 3.** Thermodynamic parameters for the biosorption of Tl(I) ions onto Fusarium sp. FP,
481 Arthrinium sp. FB and Phoma sp. FR, respectively.

482

Biosorbent	△G (kJ/mol)	△S° (J/mol K)	△H° (kJ/mol)
FP	-186.35		
FB	-179.84	15.83	126.39
FR	-176.47		

483

484

485 **Table 4:** Comparison study of inactive fungal strains (*Fusarium* sp. FP, *Arthrinium* sp. FB and
486 *Phoma* sp. FR) with other sorbents.

487

Adsorbent	pH	q_m (mg/g)	Reference
Prussian blue	7.8	5.8	32
Alginate-PB	4.0	103	33
PAAm-B	5.0	73.6	34
Modified sawdust	6–9	2.7–13.2	18
***Fusarium* sp. FP, *Arthrinium* sp. FB and *Phoma* sp. FR**	**5.0**	**94.69, 66.97 and 52.98**	**Present study**

488

489

490

491

492

493

494

Figure Legend

Figure 1: Comparative analysis of gene sequences showing the relationships between three strains and related taxa.

Figure 2: XRD spectrum of pure fungal strains before (A) and after (B) Tl(I) adsorption.

Figure 3: FT-IR spectra of pure fungal strains before (A) and after (B) Tl(I) adsorption.

Figure 4: SEM-EDS analysis of pure fungal strains (*Fusarium* sp. FP, *Arthrinium* sp. FB and *Phoma* sp. FR) and after Tl(I) adsorption.

Figure 5: XPS analytical graph of FP (a) survey scan before and after the sorption of thallium.

Figure 6: XPS analytical graph of FB (a) survey scan before and after the sorption of Tl(I) ions.

Figure 7: XPS analytical graph of FR (a) survey scan before and after the sorption of Tl(I) ions.

Figure 8: (A) Effect of pH, (B) Effect of biosorbent dose, (C) Effect of initial metal ion concentration, (D) Effect of contact time, (E) Pseudo second-order kinetic plot and (F) Langmuir isotherm plot for the sorption of Tl(I) ions onto inactive fungal strains (*Fusarium* sp. FP, *Arthrinium* sp. FB and *Phoma* sp. FR).

Figure 9: The mechanisms for Tl(I) adsorption using the strains.

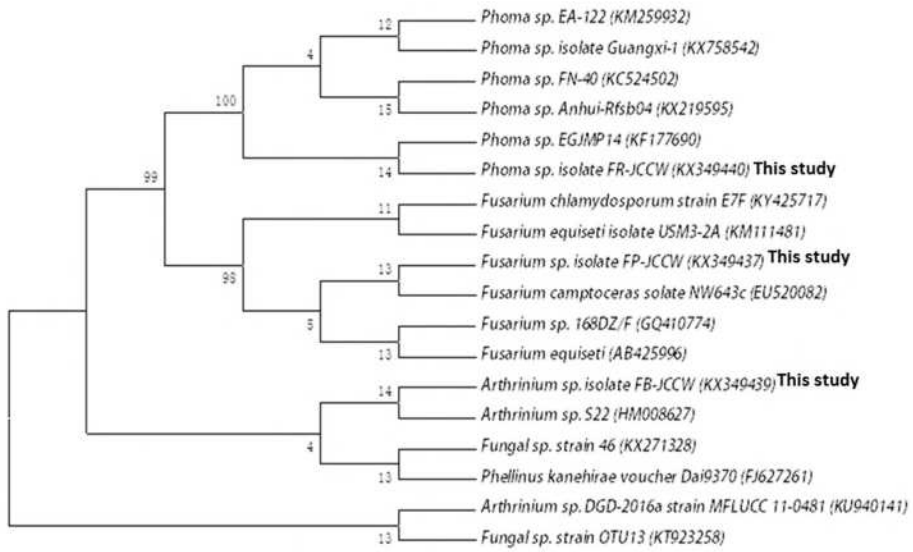
Phoma sp. EA-122 (KM259932)
Phoma sp. isolate Guangxi-1 (KX758542)
Phoma sp. FN-40 (KC524502)
Phoma sp. Anhui-Rfsb04 (KX219595)
Phoma sp. EGJMP14 (KF177690)
Phoma sp. isolate FR-JCCW (KX349440) This study
Fusarium chlamydosporum strain E7F (KY425717)
Fusarium equiseti isolate USM3-2A (KM111481)
Fusarium sp. isolate FP-JCCW (KX349437) This study
Fusarium camptoceras solate NW643c (EU520082)
Fusarium sp. 168DZ/F (GQ410774)
Fusarium equiseti (AB425996)
Arthrinium sp. isolate FB-JCCW (KX349439) This study
Arthrinium sp. S22 (HM008627)
Fungal sp. strain 46 (KX271328)
Phellinus kanehirae voucher Dai9370 (FJ627261)
Arthrinium sp. DGD-2016a strain MFLUCC 11-0481 (KU940141)
Fungal sp. strain OTU13 (KT923258)

Fig. 1.

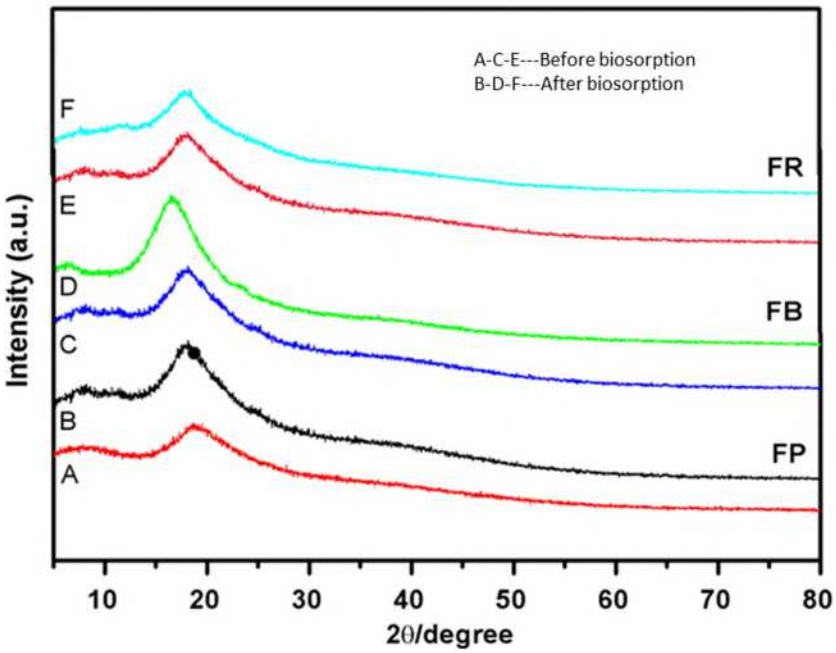
A-C-E---Before biosorption
B-D-F---After biosorption
F
E
D
C
B
A
FR
FB
FP
Intensity (a.u.)
10
20
30
40
50
60
70
80
2θ/degree

Fig. 2.

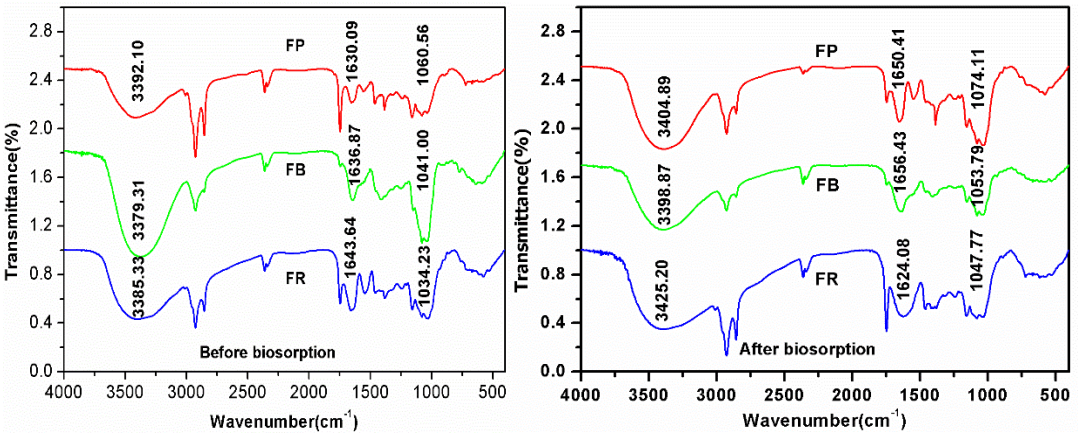
Transmittance(%)
Wavenumber(cm-1)
FP
FB
FR
3392.10
1630.09
1060.56
3379.31
1636.87
1041.00
3385.33
1643.64
1034.23
Before biosorption
3404.89
1650.41
1074.11
3398.87
1656.43
1053.79
3425.20
1624.08
1047.77
After biosorption

Fig. 3.

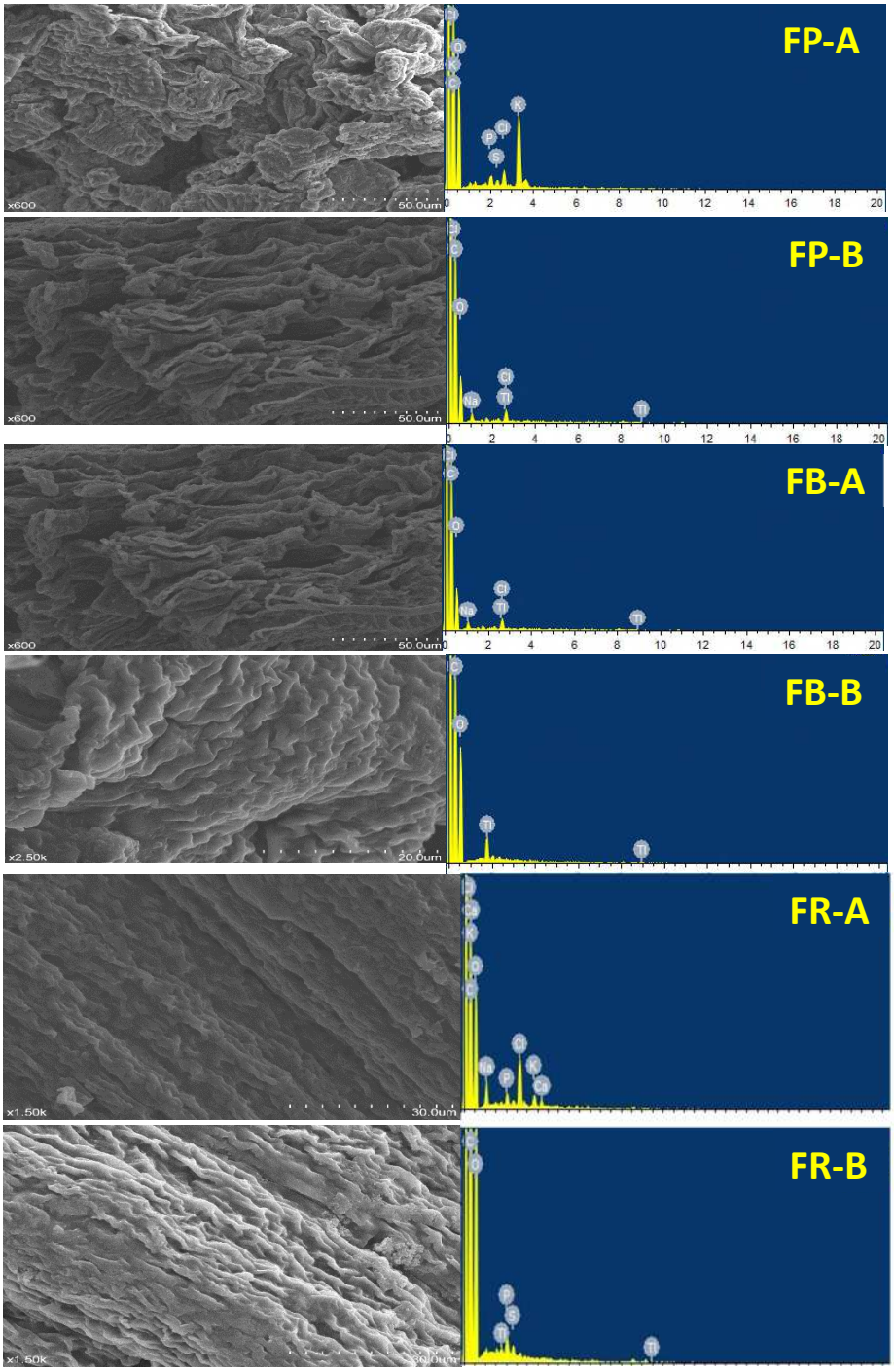

Fig 4.

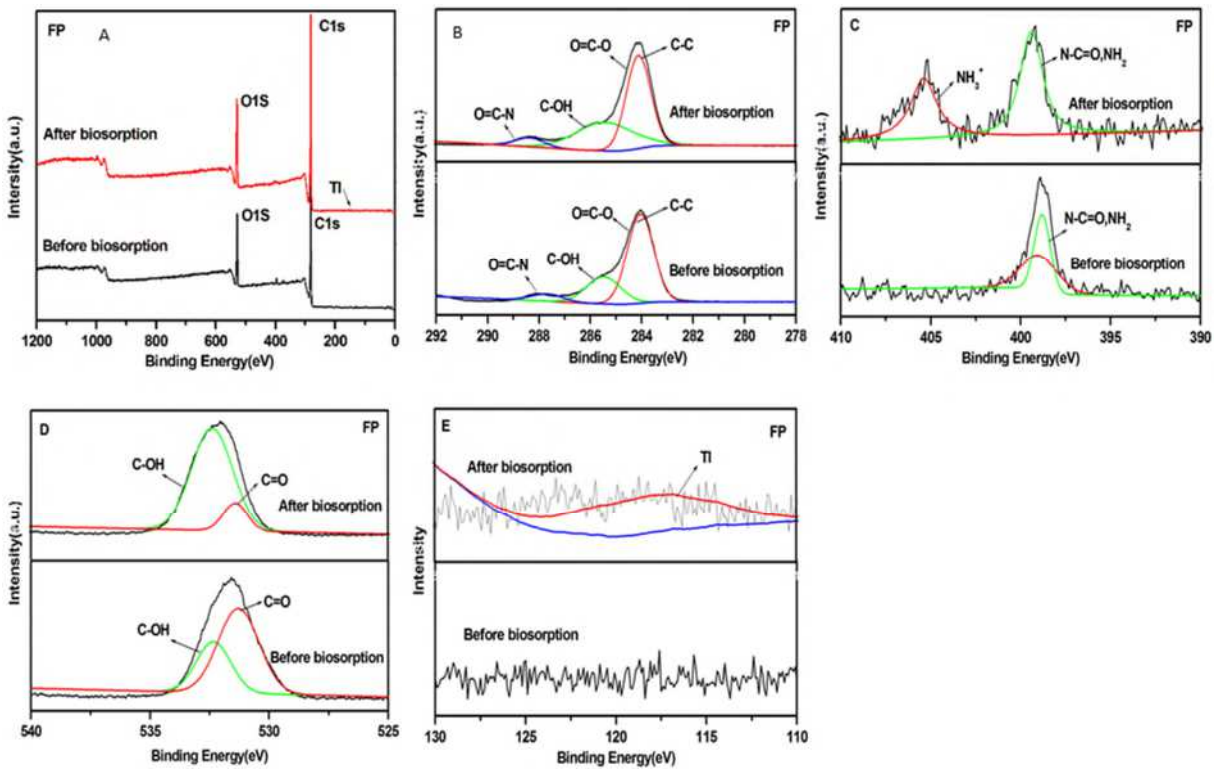
FP
A
C1s
O1S
After biosorption
Tl
O1S
C1s
Before biosorption
Intersity(a.u.)
1200 1000 800 600 400 200 0
Binding Energy(eV)
B
FP
O=C-O
C-C
O=C-N
C-OH
After biosorption
O=C-O
C-C
O=C-N
C-OH
Before biosorption
Intensity(a.u.)
292 290 288 286 284 282 280 278
Binding Energy(eV)
C
FP
NH_3^+
N-C=O,NH_2
After biosorption
N-C=O,NH_2
Before biosorption
Intensity(a.u.)
410 405 400 395 390
Binding Energy(eV)
D
FP
C-OH
C=O
After biosorption
C=O
C-OH
Before biosorption
Intensity(a.u.)
540 535 530 525
Binding Energy(eV)
E
FP
After biosorption
Tl
Before biosorption
Intensity
130 125 120 115 110
Binding Energy(eV)

Fig. 5.

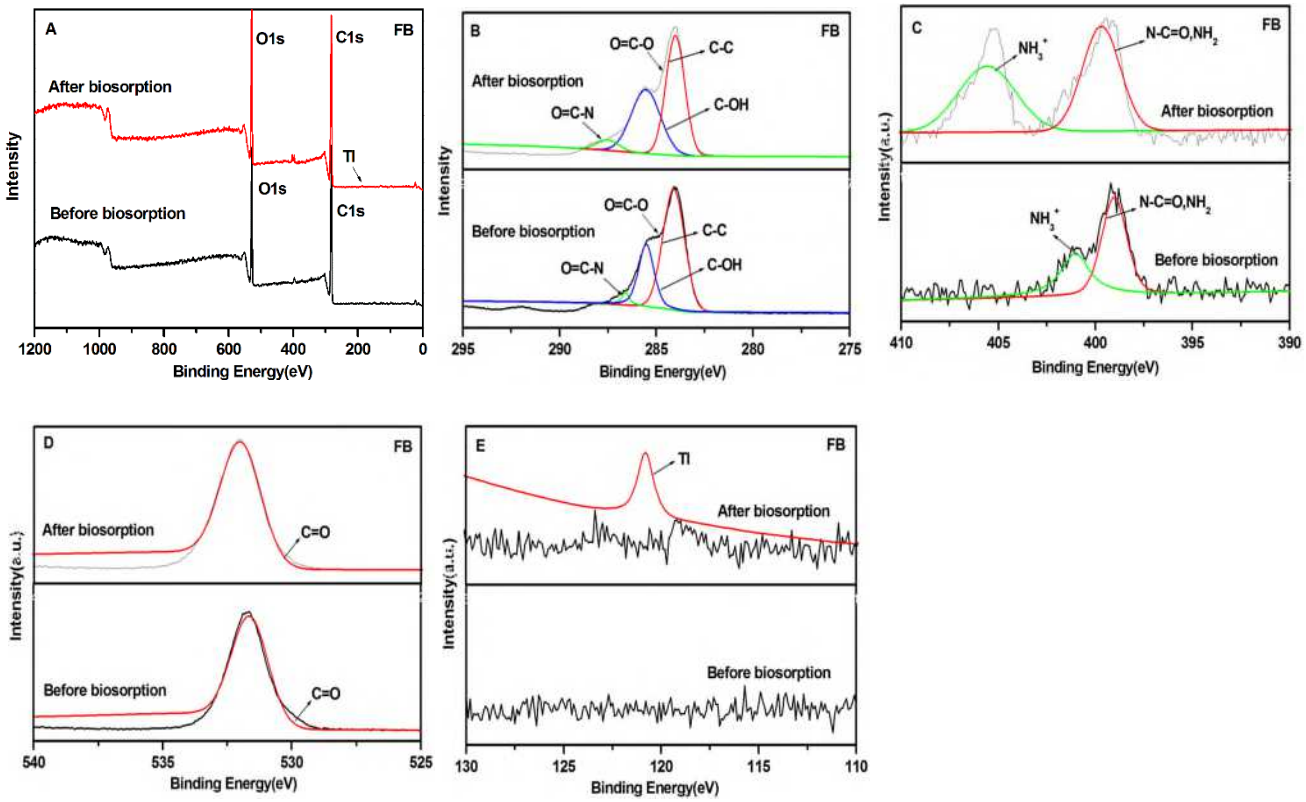
A
FB
O1s
C1s
After biosorption
Tl
O1s
C1s
Before biosorption
Intensity
1200 1000 800 600 400 200 0
Binding Energy(eV)
B
FB
O=C-O
C-C
After biosorption
O=C-N
C-OH
O=C-O
C-C
Before biosorption
O=C-N
C-OH
Intensity
295 290 285 280 275
Binding Energy(eV)
C
FB
NH3+
N-C=O,NH2
After biosorption
NH3+
N-C=O,NH2
Before biosorption
Intensity(a.u.)
410 405 400 395 390
Binding Energy(eV)
D
FB
After biosorption
C=O
Before biosorption
C=O
Intensity(a.u.)
540 535 530 525
Binding Energy(eV)
E
FB
Tl
After biosorption
Before biosorption
Intensity(a.u.)
130 125 120 115 110
Binding Energy(eV)

Fig. 6.

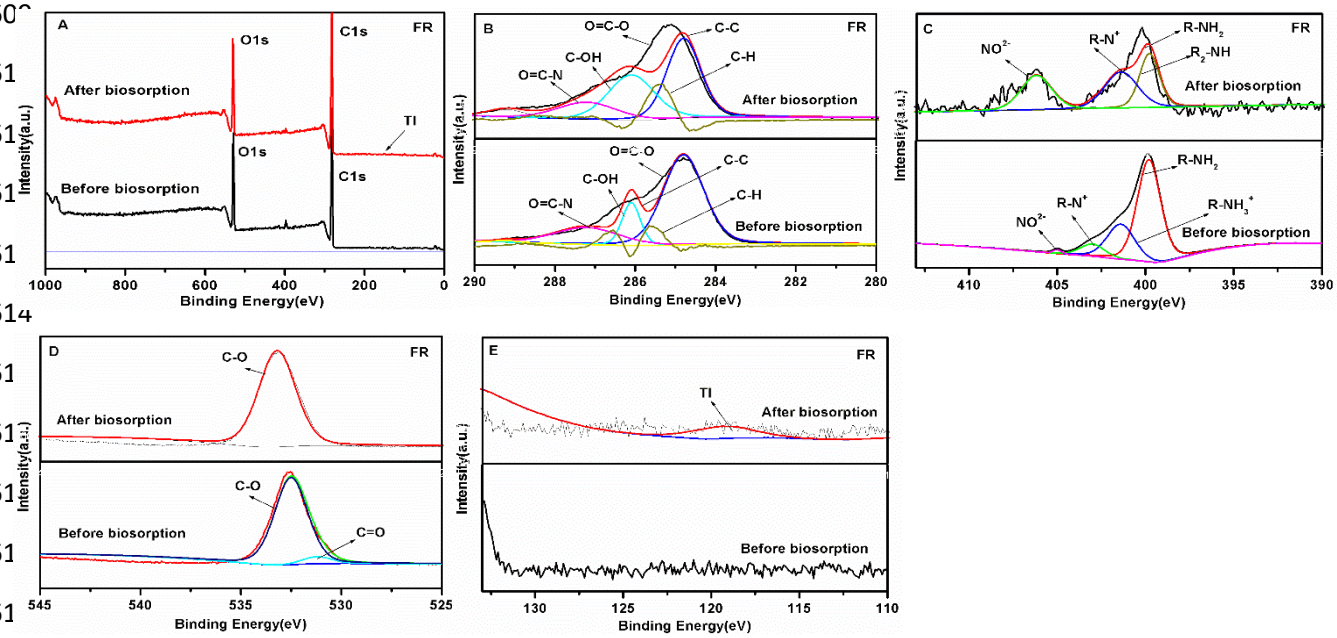
A
FR
O1s
C1s
After biosorption
TI
O1s
C1s
Before biosorption
Intensity(a.u.)
1000
800
600
400
200
0
Binding Energy(eV)
B
FR
O=C-O
C-C
C-OH
O=C-N
C-H
After biosorption
O=C-O
C-C
C-OH
O=C-N
C-H
Before biosorption
290
288
286
284
282
280
Binding Energy(eV)
C
FR
NO2-
R-N+
R-NH2
R2-NH
After biosorption
R-NH2
R-N+
NO2-
R-NH3+
Before biosorption
410
405
400
395
390
Binding Energy(eV)
D
FR
C-O
After biosorption
C-O
C=O
Before biosorption
545
540
535
530
525
Binding Energy(eV)
E
FR
TI
After biosorption
Before biosorption
130
125
120
115
110
Binding Energy(eV)

Fig. 7.

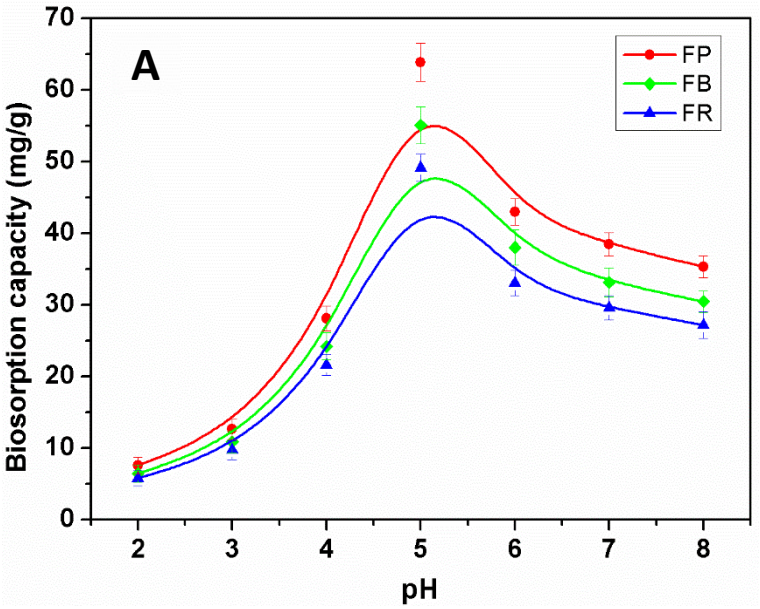
A
FP
FB
FR
Biosorption capacity (mg/g)
pH
0
10
20
30
40
50
60
70
2
3
4
5
6
7
8

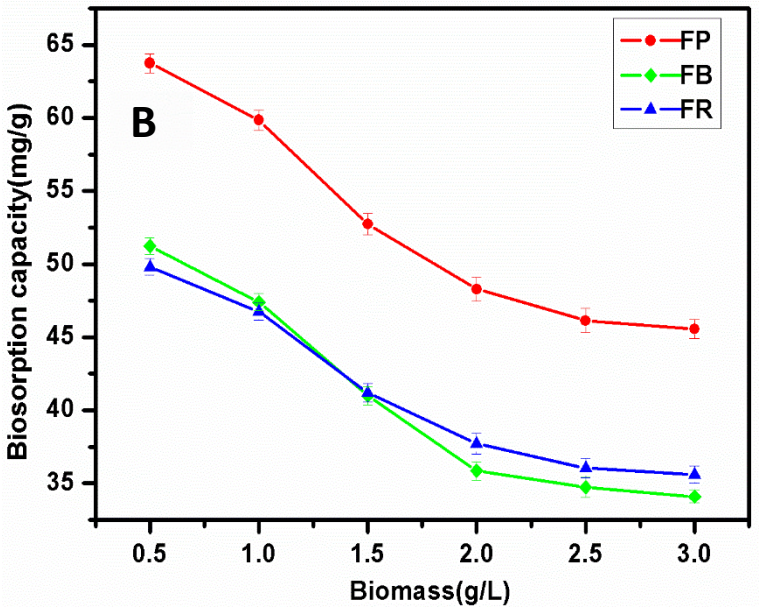
B
FP
FB
FR
Biosorption capacity(mg/g)
Biomass(g/L)
35
40
45
50
55
60
65
0.5
1.0
1.5
2.0
2.5
3.0

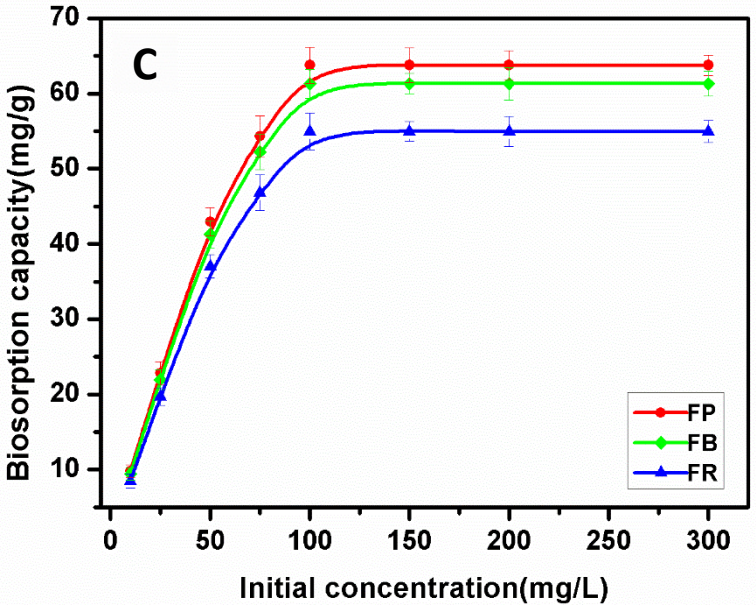
C
Biosorption capacity(mg/g)
Initial concentration(mg/L)
FP
FB
FR
0
50
100
150
200
250
300
10
20
30
40
50
60
70

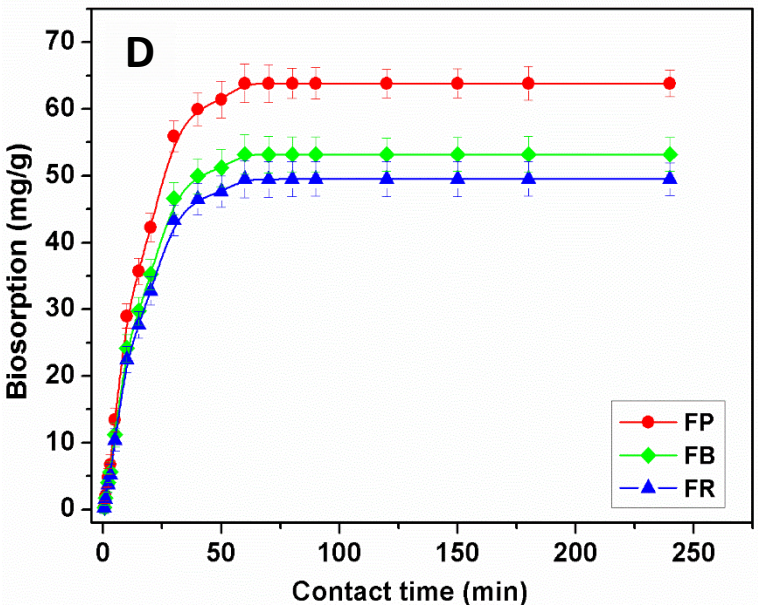
D
Biosorption (mg/g)
Contact time (min)
FP
FB
FR
0
50
100
150
200
250
0
10
20
30
40
50
60
70

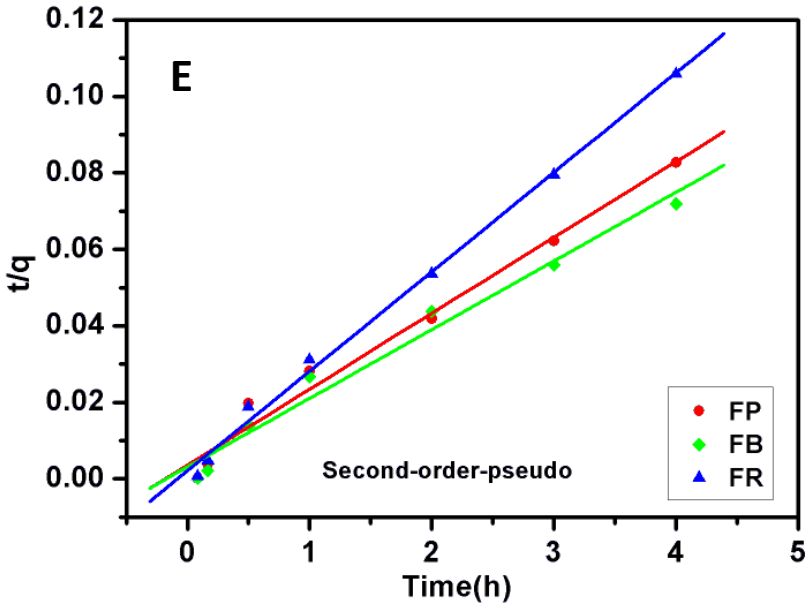
E
0.12
0.10
0.08
0.06
0.04
0.02
0.00
t/q
0
1
2
3
4
5
Time(h)
Second-order-pseudo
FP
FB
FR

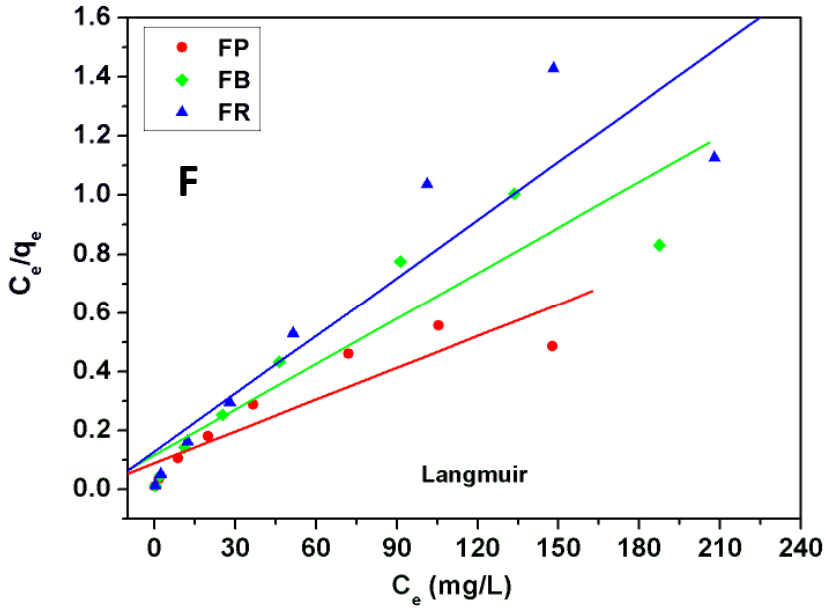
F
FP
FB
FR
1.6
1.4
1.2
1.0
0.8
0.6
0.4
0.2
0.0
C_e/q_e
0
30
60
90
120
150
180
210
240
C_e (mg/L)
Langmuir

Fig. 8A-F.

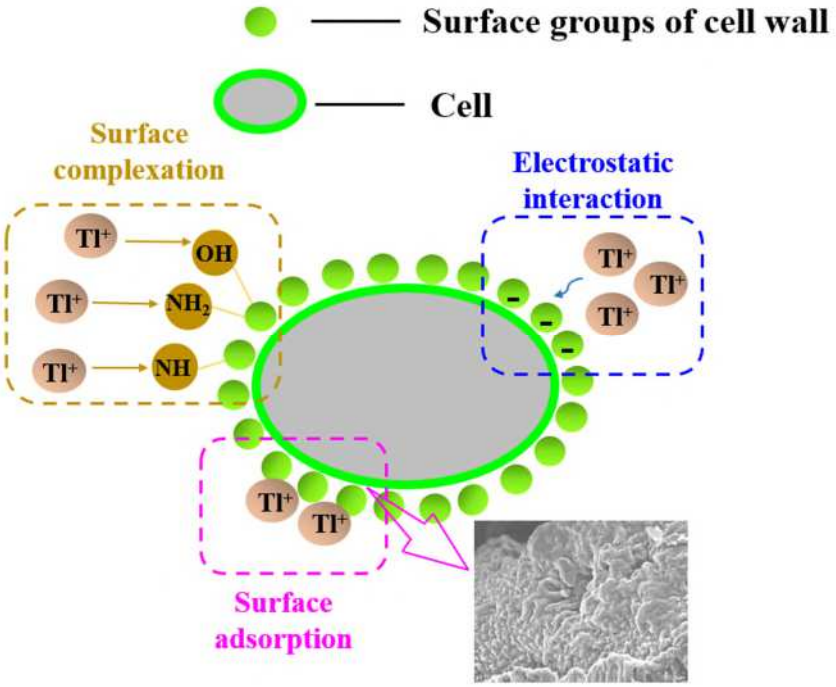

680

681 **Fig. 9.**

682

683